Accuracy of the Faddeev Random Phase Approximation for Light Atoms

C. Barbieri [*] [†]
Department of Physics, Faculty of Engineering and Physical Sciences, University of Surrey, Guildford, Surrey GU2 7XH, UK and
Theoretical Nuclear Physics Laboratory, RIKEN Nishina Center, 2-1 Hirosawa, Wako, Saitama 351-0198 Japan

D. Van Neck and M. Degroote
Center for Molecular Modeling, Ghent University, Technologiepark 903, B-9052 Gent, Belgium
(Dated: October 27, 2010)

The accuracy of the Faddeev random phase approximation (FRPA) method is tested by calculating the total and ionization energies of a set of light atoms up to Ar. Comparisons are made with the results of coupled-cluster singles and doubles (CCSD), third-order algebraic diagrammatic construction [ADC(3)], and with the experiment. It is seen that even for two-electron systems, He and Be^{2+}, the inclusion of RPA effects leads to satisfactory results and therefore it does not over-correlate the ground state. The FRPA becomes progressively better for larger atomic numbers where it gives ≈5 mH more correlation energy and it shifts ionization potentials by 2-10 mH, with respect to the similar ADC(3) method. The ionization potentials from FRPA tend to reduce the discrepancies with the experiment.

PACS numbers: 31.10.+z,31.15.Ar
Keywords: Green's function theory; ab-initio quantum chemistry; ionization energies

I. INTRODUCTION

Ab-initio studies of electronic systems aim at a direct solution of the Schrödinger equation in terms of the underlying Coulomb interaction, thus avoiding phenomenological input [1]. Most contemporary investigations of molecular and atomic systems employ the coupled-cluster (CC) method [2] due to its favorable accuracy and the gentle scaling of computational requirements with increasing number of particles. One can thus calculate molecules for which full configuration interaction (FCI) would not be feasible. Another approach with analogous characteristics is the Green's function (GF) theory (or, equivalently, propagator theory) [3–6]. An early scheme based on this approach is the outer-valence GF (OVGF) [7, 8] which expands ionization energies up to third order in perturbation theory. The OVGF is very practical and computationally simple, and it has found several applications to studies of ionization spectra [8–12]. However, it becomes inaccurate whenever inner and outer-valence ionization energies (IEs) are subject to shake-up contaminations [13–15]. In such cases one needs to resort at least to the third-order algebraic diagrammatic construction [ADC(3)] method [16, 17]. The ADC(n) approach is an intermediate state representation [18, 19] of the GF made to be consistent with perturbation theory up to order n. Thus, it is size consistent and can be systematically improved by going to higher orders. For the one-body propagator, ADC(3) implies to perform explicit configuration mixing between valence electrons and shake-up configurations such as two-hole–one-particle (2h1p) and/or two-particle–one-hole (2p1h) [21]. These states are mixed together by ADC(3) theory in a Tamm-Dancoff approximation (TDA) fashion. The accuracy of the ADC(3) approach has been tested in several studies for both IEs [20, 21] and excited states [22, 23].

Green's function theory has also extensive applications to solid states physics where the most successful scheme is the *GW* approximation (GWA) [24–26]. The GWA describes the modification of electrons through repeated interactions with collective particle-hole (ph) excitations of the system, which are described in the random phase approximation (RPA). The RPA is essential for extended systems because it screens the Coulomb interaction at large distances [5, 6]. Thus, it guarantees finite correlation energies in metals and the uniform electron gas [27–30]. In contrast, the TDA plasmon spectrum is incorrect and even diverges at small momenta. The GWA, however, is not always satisfactory. As an example two-particle (pp) or two-hole (hh) configurations—that would be included by ADC(3) but not in GWA—are necessary to explain satellite structures above and below the Fermi surface [31]. How to include these effects efficiently in GWA is still being researched [32]. Conversely, the inclusion of RPA in atomic and molecular studies may be advantageous for describing long-range (van der Waals) forces and dissociation processes [33–35]. Thus, a practical method that combines ADC(3) with RPA might become beneficial to the fields above.

In a recent publication we have considered the *ab-initio* calculation of the Ne atom using Green's function theory in the so-

[*] Present address: University of Surrey, Guildford, GU2 7XH, UK
[†] Electronic address: c.barbieri@surrey.ac.uk

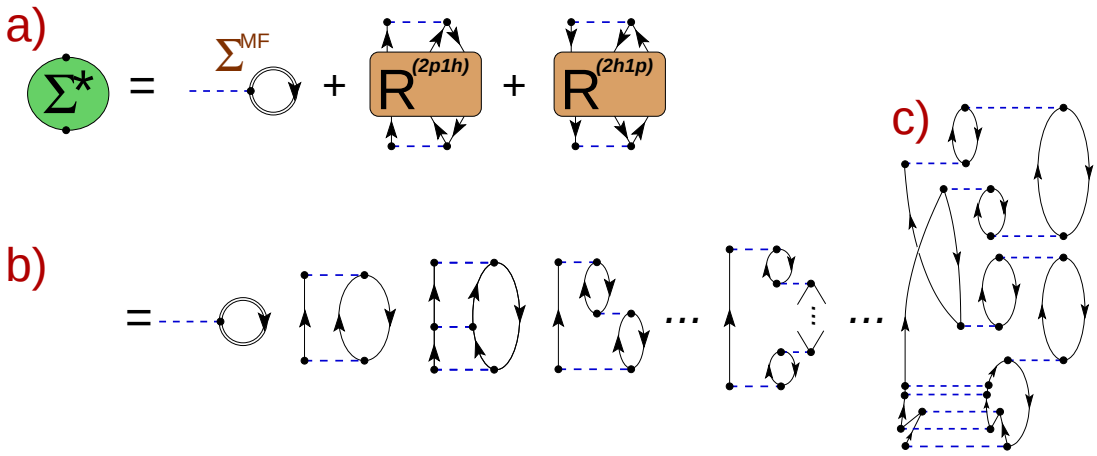

FIG. 1: The self-energy $\Sigma^\star(\omega)$ separates exactly into a mean-field term, Σ^{MF}, and the polarization propagators $R^{(2p1h/2h1p)}(\omega)$ for the 2p1h/2h1p motion, as shown in a). Upon expansion of $R(\omega)$ in Feynman diagrams, one obtains the series of diagrams b) for the self-energy. The diagram c) is another—more complicated—term appearing in the expansion of $R^{(2p1h)}(\omega)$. This is also included in the FRPA contribution of Fig. 3 but it introduces a time ordering not generated by FTDA/ADC(3). Dashed lines are antisymmetrized Coulomb matrix elements $V_{\alpha\beta,\gamma\delta}$, single lines represent the reference state (a HF propagator), and the double lines represent the correlated propagator of Eq. (1). All diagrams are time ordered, with time propagating upward.

called Faddeev random phase approximation (FRPA) [36], which was originally proposed for studies of nuclear structure [37–41] This approach completely includes 2p1h and 2h1p states in the self-energy but expands these configurations in terms of couplings between valence particles and (simpler) ph and pp/hh excitations that are calculated using RPA. By calculating these excitations in TDA one is led back to the ADC(3) scheme. Stated otherwise, the FRPA can be seen as an extension of ADC(3) that employs RPA for pairs of electron and hole excitations (see also Ref. [42] for a discussion). The inclusion of RPA opens a possible way for treating long-range correlations in both finite and extended electron systems on a equal footing. Yet, there remain a number of issues that need to be addressed before this approach can be made useful for electronic structure calculations. First, it is not guaranteed *a priory* that this method will perform equally well as the ADC(3) for few-electron cases: while Pauli correlations are fully included up to 2p1h/2h1p level, the use of RPA still includes violations for more complex excitations. Instabilities and self-screening problems induced by RPA may become more evident in light systems [32]. Moreover, the conclusions of Ref. [36] were based on calculations made for only one system (the Ne atom) and the single particle basis was not optimized to guarantee the full convergence of core electrons. Hence, a deeper investigation of its accuracy is still in order. Second, the inclusion of Pauli exchange at the 2p1h/2h1p level introduces technical complications with respect to the standard GWA approach and suitable computational schemes will need to be developed for applications to extended systems. This work addresses the first question by applying FRPA to a set of light atoms and using correlation consistent bases for extrapolating to the basis set limit.

The essential features of FRPA are reviewed in Sec. II, for the paper to be self-contained. References to the details of the formalism are also given. In our calculations we adopt gaussian basis sets and discuss the accuracy of extrapolations to the basis set limit in Sec. III A. The results for total energies and IEs are given in Sec. III B and the major conclusions are summarized in Sec. IV.

II. FORMALISM

In the present study we consider the calculation of the single-particle propagator [4, 6],

$$g_{\alpha\beta}(\omega) \;=\; \sum_n \frac{(z^n_\alpha)^* z^n_\beta}{\omega - \varepsilon^+_n + i\eta} \;+\; \sum_k \frac{z^k_\alpha (z^k_\beta)^*}{\omega - \varepsilon^-_k - i\eta}\,, \tag{1}$$

where α, β, ..., label a complete orthonormal basis and

$$\begin{aligned} z^n_\alpha &= \langle \Psi^{N+1}_n | c^\dagger_\alpha | \Psi^N_0 \rangle\,, \qquad \varepsilon^+_n = E^{N+1}_n - E^N_0\,, \\ z^k_\alpha &= \langle \Psi^{N-1}_k | c_\alpha | \Psi^N_0 \rangle\,, \qquad \varepsilon^-_k = E^N_0 - E^{N-1}_k\,. \end{aligned} \tag{2}$$

In these definitions, c_α ($c^\dagger_\beta$) are second quantization destruction (creation) operators, $|\Psi^{N+1}_n\rangle$, $|\Psi^{N-1}_k\rangle$ are the eigenstates, and E^{N+1}_n, E^{N-1}_k the eigenenergies of the $(N \pm 1)$-electron system. Therefore, the poles of the propagator reflect the electron affinities

(EAs) and IEs. Eq. (1) also yields the total binding energy via the Migdal-Galitskiĭ-Koltun sum rule [6],

$$E_0^N = \frac{1}{2}\sum_k \sum_{\alpha,\beta} \left(u_{\alpha\beta} + \varepsilon_k^- \delta_{\alpha\beta}\right) z_\beta^k (z_\alpha^k)^* \tag{3}$$

where $u_{\alpha\beta}$ represent the matrix elements of the one-body part of the hamiltonian (kinetic energy plus nuclear attraction) and the k-sum runs only over the eigenstates of the (N-1)-electron systems.

The one-body Green's function solves the Dyson equation (from hereafter, summations over repeated indices are implied)

$$g_{\alpha\beta}(\omega) \;=\; g^0_{\alpha\beta}(\omega) \;+\; g^0_{\alpha\gamma}(\omega)\,\Sigma^\star_{\gamma\delta}(\omega)\,g_{\delta\beta}(\omega) \;\;, \tag{4}$$

where $g^0(\omega)$ is the propagator for a free particle. The irreducible self-energy $\Sigma^\star_{\gamma\delta}(\omega)$ acts as an effective, energy-dependent, potential that can be written as [43, 44]

$$\begin{aligned}\Sigma^\star_{\alpha\beta}(\omega) \;&=\; \Sigma^{MF}_{\alpha\beta} \;+\; \tilde{\Sigma}_{\alpha\beta}(\omega) \\ &=\; \int \frac{d\omega}{2\pi i}\, V_{\alpha\gamma,\beta\delta}\, g_{\delta\gamma}(\omega)\, e^{-i\omega\eta^+} \;+\; \frac{1}{4} V_{\alpha\lambda,\mu\nu}\left[R^{(2p1h)}_{\mu\nu\lambda,\mu'\nu'\lambda'}(\omega) \;+\; R^{(2h1p)}_{\mu\nu\lambda,\mu'\nu'\lambda'}(\omega)\right] V_{\mu'\nu',\beta\lambda'} \;\;,\end{aligned} \tag{5}$$

and $V_{\alpha\beta,\gamma\delta}$ are antisymmetrized Coulomb matrix elements. In Eq. (5) we have emphasized the mean-field (MF) contribution to the self-energy. This generalizes the Hartree-Fock (HF) potential by replacing the Slater MF with the (correlated) density matrix extracted from the dressed propagator (1). The Σ^{MF} is represented by the first diagram on the right hand side in Figs. 1a) and 1b). The remaining term, $\tilde{\Sigma}(\omega)$, accounts for deviations from the mean-field and depends on the 2p1h and 2h1p polarization propagators, $R^{(2p1h)}(\omega)$ and $R^{(2h1p)}(\omega)$. These involve the simultaneous propagation of 2p1h (or 2h1p) *and higher* excitations. Eq. (5) is represented in Fig.1a) in terms of Feynman diagrams. The $R(\omega)$ can also be expanded in terms of Coulomb matrix elements and unperturbed propagators, as shown in Figs. 1b) and 1c).

A. The Faddeev random phase approximation method

The Faddeev approach consists in expanding $R^{(2p1h)}$ and $R^{(2h1p)}$ in terms of couplings between single electrons or holes and ph, pp or hh excitations [36, 45]. Information about the latter is fully contained in the ph polarization propagator that describes excited states of the N-electron system

$$\begin{aligned}\Pi_{\alpha\beta,\gamma\delta}(\omega) \;&=\; \sum_{n\neq 0} \frac{\langle\Psi^N_0|c^\dagger_\beta c_\alpha|\Psi^N_n\rangle\,\langle\Psi^N_n|c^\dagger_\gamma c_\delta|\Psi^N_0\rangle}{\omega - \left(E^N_n - E^N_0\right) + i\eta} \\ &-\; \sum_{n\neq 0} \frac{\langle\Psi^N_0|c^\dagger_\gamma c_\delta|\Psi^N_n\rangle\,\langle\Psi^N_n|c^\dagger_\beta c_\alpha|\Psi^N_0\rangle}{\omega + \left(E^N_n - E^N_0\right) - i\eta} \;\;,\end{aligned} \tag{6}$$

and the two-particle propagator that describes the addition/removal of two electrons

$$\begin{aligned}g^{II}_{\alpha\beta,\gamma\delta}(\omega) \;&=\; \sum_{n} \frac{\langle\Psi^N_0|c_\beta c_\alpha|\Psi^{N+2}_n\rangle\,\langle\Psi^{N+2}_n|c^\dagger_\gamma c^\dagger_\delta|\Psi^N_0\rangle}{\omega - \left(E^{N+2}_n - E^N_0\right) + i\eta} \\ &-\; \sum_{k} \frac{\langle\Psi^N_0|c^\dagger_\gamma c^\dagger_\delta|\Psi^{N-2}_k\rangle\,\langle\Psi^{N-2}_k|c_\beta c_\alpha|\Psi^N_0\rangle}{\omega - \left(E^N_0 - E^{N-2}_k\right) - i\eta} \;\;.\end{aligned} \tag{7}$$

These Green's functions are calculated as resummations of ring and ladder diagrams using either the TDA or the RPA,

$$\Pi^{(TDA/RPA)}_{\alpha\beta,\gamma\delta}(\omega) \;=\; \Pi^{0\,(TDA/RPA)}_{\alpha\beta,\gamma\delta}(\omega) \;+\; \Pi^{0\,(TDA/RPA)}_{\alpha\beta,\mu\nu}(\omega)\, V_{\mu\eta,\nu\rho}\, \Pi^{(TDA/RPA)}_{\rho\eta,\gamma\delta}(\omega)\,, \tag{8}$$

$$g^{II\,(TDA/RPA)}_{\alpha\beta,\gamma\delta}(\omega) \;=\; g^{0\,(TDA/RPA)}_{\alpha\beta,\gamma\delta}(\omega) \;+\; \frac{1}{4}\, g^{0\,(TDA/RPA)}_{\alpha\beta,\mu\nu}(\omega)\, V_{\mu\nu,\rho\eta}\, g^{II\,(TDA/RPA)}_{\rho\eta,\gamma\delta}(\omega)\,. \tag{9}$$

The difference between the two approximations is in the choice of the propagators for non the interacting ph (Π^0) and pp/hh (g^0) configurations. Both of these contain a term that conserves the direction of time propagation and one that inverts it. By including only the first term the TDA equations are obtained. If both contributions are retained, one is led to the RPA. The RPA induces extra time orderings in the resummations of Eqs. (8) and (9) as shown in Fig. 2 for the ph case. These account for 2p2h and more complicated admixtures in the ground state that are generated by correlations.

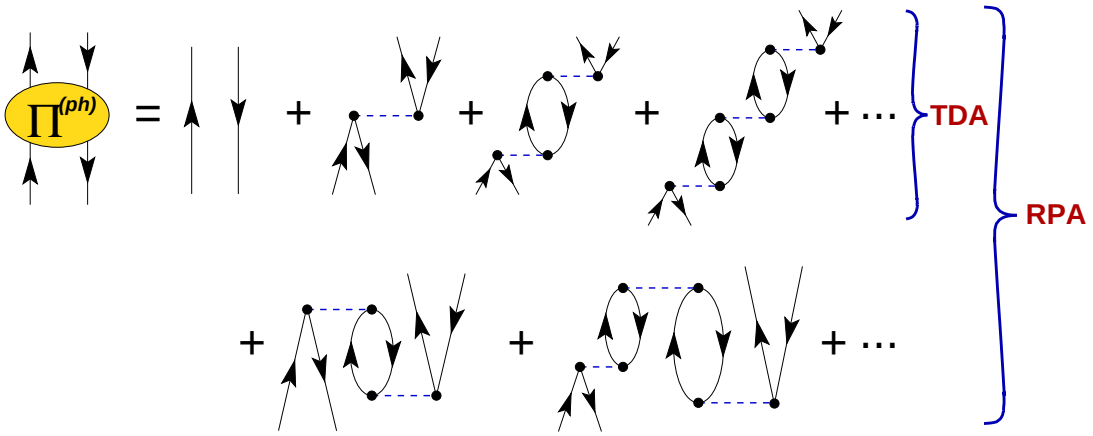

FIG. 2: Expansion of the ph propagator $\Pi(\omega)$ in a series of ring diagrams. The diagrams resummed by TDA are shown in the first line. The second line gives examples of time-inversion patterns that are generated only by RPA, these account for the presence of 2p2h and more complicated configurations in the correlated ground state. The diagrams are time ordered, with time propagating upward.

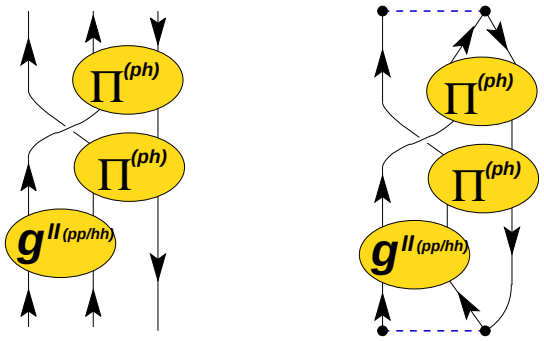

FIG. 3: *Left:* Example of one of the diagrams for $R^{(2p1h)}(\omega)$ that are summed to all orders by means of the Faddeev method. Each of the ellipses represent an infinite sum of rings [$\Pi(\omega)$] or ladders [$g^{II}(\omega)$], as generated by Eqs. (8) and (9). Contributions of all possible partial waves are included. *Right:* The corresponding contribution to the self-energy, obtained upon insertion of $R^{(2p1h)}(\omega)$ into Eq. (5). This representation is valid for both the FTDA and FRPA approaches, the difference between the two being in the diagrams implicitly resummed inside $\Pi(\omega)$ and $g^{II}(\omega)$ (see Fig. 2).

The $R^{(2p1h)}(\omega)$ and $R^{(2h1p)}(\omega)$ propagators are obtained by first calculating Π and g^{II} and then by recoupling them to single electron or hole states, as shown in Fig. 3. This is done by solving the set of Faddeev equations detailed in Refs. [36, 45]. We refer to this procedure as Faddeev TDA (FTDA) or Faddeev RPA depending on the approximation chosen to solve Eqs. (8) and (9). The Faddeev summation and the diagram depicted in Fig. 3 are the same in both cases. Contributions from ph, pp and hh excitations in all possible partial waves are included in FRPA/FTDA since this is required for a complete solution of the problem. In order to fulfill Pauli constraints up to 2p1h and 2h1p level in the expansion for $R(\omega)$ one must employ the generalized version of RPA (in which the Coulomb matrix elements are the antisymmetrized ones). Two separate sets of Faddeev equations are used for $R^{(2p1h)}(\omega)$ and $R^{(2h1p)}(\omega)$.

The Faddeev procedure can be recast in terms of two diagonalizations in the 2p1h and the 2h1p configuration spaces. In each case one solves a *non-hermitian* eigenvalue problem [45]

$$\mathbf{H}_{Fd}\,\mathbf{F} \;=\; \mathbf{F}\,\mathbf{E}_{Fd} \qquad\qquad \mathbf{F}^{\dagger}\mathbf{F} = \mathbf{1}\,, \tag{10}$$

where $\mathbf{E}_{Fd} = diag\{E^{(n)}_{Fd}\}$ and the Faddeev hamiltonian $\mathbf{H}_{Fd}$ is constructed from the solutions of Eqs. (8) and (9). The $R^{(2p1h)}$ propagator is written in terms of the eigenvectors $\mathbf{F}^{(n)}$ and eigenenergies $E^{(n)}_{Fd}$,

$$R^{(2p1h)}_{\alpha\beta\gamma,\mu\nu\lambda}(\omega) \;=\; \sum_n \left(\mathbf{U}\,\mathbf{F}^{(n)}\right)^{(2p1h)}_{\alpha\beta\gamma} \frac{1}{\omega - E^{(n)}_{Fd} + i\eta} \left(\mathbf{F}^{(n)\dagger}\mathbf{U}^{\dagger}\right)^{(2p1h)}_{\mu\nu\lambda}\,, \tag{11}$$

and an analogous relation holds for $R^{(2h1p)}$. In Eq. (11), the matrix $U_{\alpha\beta\gamma,p_1p_2h}$ is a correction vertex chosen—in analogy with ADC(3) theory—as the minimum coupling that ensures consistency with perturbation theory up to third order. When contracted

with $V_{\alpha\lambda,\mu\nu}$ in Eq. (5), it reproduces exactly the same effective coupling amplitudes of ADC(3) [17]. The explicit form of the FTDA/FRPA equations is given in Ref. [36] and their reduction to a matrix diagonalization (10) is described in [45].

Inserting Eq. (11) into (5) and (4), the Dyson equation is transformed into a diagonalization problem

$$\varepsilon \begin{pmatrix} \mathbf{z} \\ \mathbf{w}_{2p1h} \\ \mathbf{w}_{2h1p} \end{pmatrix} = \begin{pmatrix} \mathbf{\Sigma}^{MF} & \left(\mathbf{U}^\dagger \mathbf{V}^\dagger\right)_{2p1h} & \left(\mathbf{U}^\dagger \mathbf{V}^\dagger\right)_{2h1p} \\ (\mathbf{VU})_{2p1h} & \left(\mathbf{F}\,\mathbf{E}_{Fd}\,\mathbf{F}^\dagger\right)_{2p1h} & 0 \\ (\mathbf{VU})_{2h1p} & 0 & \left(\mathbf{F}\,\mathbf{E}_{Fd}\,\mathbf{F}^\dagger\right)_{2h1p} \end{pmatrix} \begin{pmatrix} \mathbf{z} \\ \mathbf{w}_{2p1h} \\ \mathbf{w}_{2h1p} \end{pmatrix}, \tag{12}$$

$$\|\mathbf{z}\|^2 + \|\mathbf{w}_{(2p1h)}\|^2 + \|\mathbf{w}_{(2h1p)}\|^2 = 1 ,$$

which can be solved directly for the IE and EA, $\varepsilon^{+/-}$, and the corresponding residues, z_α, in the single particle propagator (1). In the particular case of the FTDA, one finds that the Faddeev hamiltonian is hermitian and is equivalent to the same effective interaction among 2p1h or 2h1p states in ADC(3). In this case $\mathbf{H}_{FTDA} = \mathbf{F}\mathbf{E}_{FTDA}\mathbf{F}^\dagger$ and Eq. (12) reduces to the usual Dyson ADC(3) matrix.

III. RESULTS

We considered a set of neutral atoms and ions corresponding to shell- and subshell-closures with Z≤18. The calculations of the smallest systems (He, Be and Be^{2+}) were performed using the correlation-consistent polarization valence gaussian bases, cc-pVXZ, of increasing quality from double- to quintuple-zeta (X=2-5). For the larger atoms it was found that a sizable fraction of the correlation energy is lost with similar bases. The remaining systems were therefore calculated with the corresponding core-valence bases, cc-pCVXZ, which include additional compact gaussians to improve the description of the core electrons. This choice was seen to speed up the convergence and led to accurate results for these atoms [55]. The correction to the correlation energies induced by the extra core orbits increases with the number of electrons and it was found to be ≈40 mH for Ne and ≈300 mH for Mg, in the cc-pCVQZ basis.

The bases for the Be^{2+} (Mg^{2+}) ions were obtained from the cc-p(C)VXZ sets for He (Ne) but scaling the corresponding single-particle orbits to correct for the different atomic number,

$$\phi^i_{\mathrm{Be}^{2+}/\mathrm{Mg}^{2+}}(r) \;\propto\; \phi^i_{He/Ne}(r\frac{Z}{N}) \tag{13}$$

where Z is the nuclear charge and N=Z-2 the number of electrons.

Correlation and ionization energies were computed with both the FTDAc/ADC(3)c and the FRPAc methods. In this notation, the letter 'c' indicates the self-consistent treatment of the sole MF diagram in the self-energy. This means that Σ^{MF} was derived by iterating Eq. (4) and the first term on the right hand side in (5) [the first diagram in Figs. 1a) and 1b)]. In other words, Σ^{MF} is renormalized by evaluating it directly in terms of the fully correlated propagator, instead of the reference state. This aspect is important since it consistently includes all the perturbation theory contributions up to third-order and more. The dynamic part of the self-energy $\tilde{\Sigma}(\omega)$ was instead calculated in terms of a HF reference state. The ground-state energies were also compared to the results of CC singles and doubles (CCSD) theory, starting from the same HF reference state.

A. Convergence

Total binding energies predicted by both Green's function theory and CCSD are compared with the results of full configuration interaction (FCI) in Table. I. For Ne atom in cc-pCVDZ, Green's functions and CCSD agree with each other and deviate from the exact result by less than 2 mH. FRPA gives just a very small correction but it halves the discrepancy between FTDA and FCI. The total correlation energy for this basis is 233 mH. The atom of Be is the most difficult case among those discussed here due to the fact that this is not a good closed-shell system. In this case, a near degeneracy between the 2s and 2p orbitals leads to very soft excitations of the $J^\pi=1^-$, S=1 states and drives the ph-RPA equations close to instability. The FRPA was thus solved by employing the TDA approximation of the polarization propagator, Eq.(6), in this channel alone (all other partial waves were treated properly in RPA). The resulting correlation energies agree with FTDAc/ADC(3)c, indicating that RPA is not crucial for this small system, but neither does it introduce spuriosities by over-correlating the ground state. FCI calculations of Be were possible for all bases up to quintuple-zeta and are reproduced by CCSD with high accuracy. However, FTDAc/ADC(3)c and FRPAc are consistently behind by about 9 mH, corresponding to 10% of the total correlation energy. This is the most serious discrepancy obtained in this work and suggests a limitation of the FRPA—in its present form—for near-degenerate systems.

To overcome this, it may be necessary to introduce self-consistency in the polarization propagator $R(\omega)$, to account for orbit relaxation, or to improve the treatment of the excitation spectrum of the polarization propagator beyond bare ph states [46] [56]. The close agreement between FTDAc/ADC(3)c and FRPAc in Table. I is a welcome feature since for a few electrons in the Be atom one should expect RPA-like effects (that is, several ph excitations admixed in the ground state) to be negligible. The RPA is not optimal for few-body systems since breaking of the Pauli principle may become substantial in these cases. Nevertheless, this result (and the one for He discussed below) suggests that it can be safely applied also in this regime without overestimating ground-state correlations. The usual issues of RPA for cases of near degeneracy remain and may lead to instabilities in certain partial waves, as described above. In the worst case it is still possible to release the RPA requirement in such channels and obtain reasonable results.

Extrapolations to the basis set limit were obtained from two consecutive sets according to

$$E_X = E_\infty + AX^{-3} \,, \tag{14}$$

where X is the cardinal number of the basis. This relation is known to give proper extrapolations for correlation energies [1]. Table II gives some examples of the calculated binding energies for all basis sizes and shows the convergence of the extrapolated results. In the smallest systems, up to Ne, we find changes of less than 2 mH between the last two extrapolations (X=T,Q and X=Q,5). This number can be taken as a measure of the uncertainty in reaching the basis set limit. For the larger atoms Mg is the one that converges more slowly, with a difference of 10 mH (we found 7 mH for Ar). Calculations with X=6 are beyond present computational capabilities. However, given the fast convergence with increasing cardinal number, it appears safe to assume an uncertainty of $\leq$5 mH for Mg and Ar.

In general, IEs and EAs tend to converge faster because they represent differences of total energies between the N-electron ground state and the excited states of (N±1) electrons. Inaccuracies in the correlation energies are similar and therefore could cancel each other to a large extent. Eq. (14) is preserved when taking differences of correlation energies that obey the same trend and therefore one may expect that a similar behaviour applies to IEs for large basis sets. However, this is not always guaranteed especially in cases where shakeup configurations are important. For smaller bases these contributions are less stable with respect to changing basis set and can affect IEs differently. The possible behaviours are displayed in Table. II for the calculated IEs of Ar. The 3p orbit has a strong one-hole character and converges smoothly. Here, the difference of only 0.4 mH between the last two extrapolations indicates that a convergence as X^{-3} effectively takes place. We obtained similar trends for the other cases. The only remarkable exception is the 3s hole in Ar which has a large admixture of 2h1p configurations. The calculated IE shows an oscillatory behaviour, however, a monotonic convergence could still happen for larger bases, once shakeup contributions have stabilized. In Sec. III B, we will apply Eq. (14) also to extrapolate ionization energies. We estimate an error up to 2 mH for the larger atoms and <1 mH for the smaller ones.

$E_{\rm tot}$	Ne	Be			
	cc-pCVDZ	cc-pVDZ	cc-pVTZ	cc-pVQZ	cc-pV5Z
ADC(3)c/FTDAc	-128.7191	-14.6089	-14.6154	-14.6314	-14.6375
FRPAc	-128.7210	-14.6084	-14.6150	-14.6310	-14.6371
CCSD	-128.7211	-14.6174	-14.6236	-14.6396	-14.6457
full CI	-128.7225	-14.6174	-14.6238	-14.6401	-14.6463

TABLE I: Total binding energies (in Hartrees) for Ne and Be obtained for cc-p(C)VXZ bases of different sizes. The results obtained with ADC(3)c and FRPAc (with self-consistency in the MF diagram) and with the CCSD methods are compared to FCI calculations.

B. Ground states and ionization energies of simple atoms

Table III shows the ground state energies extrapolated from X=Q,5 for both Green's function and CCSD methods. These are compared to the corresponding Hartree-Fock results and the experiment. The empirical values are from Refs. [47–49] and have been corrected by subtracting relativistic effects. The CCSD results for He and Be^{2+} are equivalent to FCI, from which we see that FRPAc misses 1 mH, or 2%, of the correlation energy of He. In larger systems FRPAc explains at least 99% of the correlation energies and all calculations, including CCSD, agree with the experiment within the uncertainty expected from basis extrapolation. For Z$\geq$10, the inclusion of RPA correlations predicts about 5 mH more binding than the corresponding FTDAc/ADC(3)c. The atom of Be is the only exception to this trend as already noted above. In this case the 9 mH difference between FRPAc and CCSD is seen also in the basis limit. Based on the agreement between FCI and CCSD in Tab.I, the remaining

			cc-p(C)VDZ	cc-p(C)VTZ	cc-p(C)VQZ	cc-p(C)V5Z	Experiment
$E_{\rm tot}$:	Be	calc.	-14.6084	-14.6150	-14.6310	-14.6371	-14.6674
		extrap.		-14.6178	-14.6427	-14.6436	
	Ne	calc.	-128.7210	-128.8643	-128.9079	-128.9226	-128.9383
		extrap.		-128.9246	-128.9397	-128.9381	
	Mg	calc.	-199.8147	-199.9507	-200.0033	-200.0271	-200.054
		extrap.		-200.0080	-200.0417	-200.0519	
IE:	Ar (3p)	calc.	0.5623	0.5695	0.5751	0.5770	0.579
		extrap.		0.5725	0.5792	0.5788	
	Ar (3s)	calc.	1.0985	1.0616	1.0599	1.0622	1.075
		extrap.		1.0461	1.0586	1.0646	

TABLE II: Convergence of total energies and IEs (in Hartrees) in the FRPAc approach. First lines: energies calculated using double (X=D) to quintuple (X=5) valence orbits basis sets. Second lines: results extrapolated from two consecutive sets using Eq. (14). The Be atom was calculated with the cc-pVXZ bases, while Ne, Mg and Ar were done using cc-pCVXZ. The experimental values are from Refs. [48–50].

discrepancy with the experiment (≈15 mH) may be due the basis set employed which is probably not capable to accommodate the relevant correlation effects. We have attempted FRPAc calculations with the aug-cc-pVXZ bases which should allow for a better description of the valence orbits but without any appreciable change in the results.

The Ne atom was also computed in the FRPA approach by using a Hartree-Fock basis with a discretized continuum [36]. The basis set was chosen as large as possible to approach the basis set limit for IEs and EAs but was not optimized for treating core orbits. The total binding energy obtained was 128.888 H, away from the basis set limit of Table. III and the experiment.

	Hartree-Fock	FTDAc	FRPAc	CCSD	Experiment
He	-2.8617 (+42.0)	-2.9028 (+0.9)	-2.9029 (+0.8)	-2.9039 (-0.2)	-2.9037
Be^{2+}	-13.6117 (+43.9)	-13.6559 (-0.3)	-13.6559 (-0.3)	-13.6561 (-0.5)	-13.6556
Be	-14.5731 (+94.3)	-14.6438 (+23.6)	-14.6436 (+23.8)	-14.6522 (+15.2)	-14.6674
Ne	-128.5505 (+387.8)	-128.9343 (+4.0)	-128.9381 (+0.2)	-128.9353 (+3.0)	-128.9383
Mg^{2+}	-198.83 7 (+444)	-199.226 (-5)	-199.228 (-7)	-199.225 (-4)	-199.221
Mg	-199.616 (+438)	-200.048 (+6)	-200.052 (+2)	-200.050 (+4)	-200.054
Ar	-526.820 (+724)	-527.543 (+1)	-527.548 (-4)	-527.536 (+8)	-527.544
σ_{rms} [mH]	392	9.5 (3.6)	9.5 (3.4)	6.9 (4.2)	

TABLE III: Hartree-Fock, ADC(3)c/FTDAc, FRPAc and CCSD total energies (in Hartrees) extrapolated from the cc-p(C)VQZ and cc-p(C)V5Z basis sets. He, Be^{2+} and Be where calculated with the cc-pVXZ bases, while cc-pCVXZ bases were used for the remaining atoms. The deviations from the experiment are indicated in parentheses (in mHartrees). The experimental energies are from Refs. [47–49]. The *rms* errors in parentheses are calculated by neglecting the Be results.

Ionization energies are shown in Table. IV, together with the predictions from Hartree-Fock theory and the second-order self-energy (obtained by retaining only the first two diagrams of Fig. 1b). Second-order corrections account for a large part of correlations but still lead to sizable errors. The additional correlations included in the present calculations appear to reduce this error substantially. The FTDAc/ADC(3)c results give a measure of the importance of a treatment that is consistent with at least third order perturbation theory [13]. Corrections are particularly large for states with higher ionization energies where the density of 2h1p states is increased. Since configuration mixing among these states is not introduced by strict second-order perturbation theory, calculations at least at the level of FTDAc are required in these cases. Configuration mixing among the 2h1p states reduces the errors in the 1*s* state in Be by a factor of five. Another effect is the fragmentation of the 3*s* orbit of Ar. Second-order calculations predict this as a quasiparticle state 36 mH away from the empirical energy and carrying 0.81 of the total orbit's intensity. A small satellite state with relative intensity of 0.10 is calculated at larger separation energies. The mixing

with 2h1p configurations corrects the energies of both peaks and redistributes their strengths more correctly. For the FRPAc calculation the peak at 1.065 H has intensity of 0.61, close to the experimental values (peak at 1.075 H with intensity 0.55 [50]). The second peak is obtained at 1.544 H and carries the remaining strength of the original quasiparticle.

Adding the effects of collective RPA excitations has a larger impact on ionization than on correlation energies. Almost all the calculated IEs shift closer to the experimental values by a few mH. The only exceptions are the two-electron He atom, where the RPA approach tends to overestimate correlations, and the first ionization of Be, where soft excitations tend to invalidate the RPA. In general, the *rms* error for the valence orbits of Table. IV lowers from 13.7 to 10.6 mH, passing from FTDAc to FRPAc.

The FRPAc first and second IEs of the Ne atom computed using the discretized continuum basis of Ref. [36] are 0.801 and 1.795 H. These are in good agreement with the extrapolations of Table. IV and gives us further confidence in applying Eq. (14) also for quasiparticle states.

		Hartree-Fock	(2^{nd} order)c	FTDAc/ ADC(3)c	FRPAc	Experiment [51, 52]
He	1s	0.918 (+14)	0.9012 (-2.5)	0.9025 (-1.2)	0.9008 (-2.9)	0.9037
Be^{2+}:	1s	5.6672 (+116)	5.6542 (-1.4)	5.6554 (-0.2)	5.6551 (-0.5)	5.6556
Be	2s	0.3093 (-34)	0.3187 (-23.9)	0.3237 (-18.9)	0.3224 (-20.2)	0.3426
	1s	4.733 (+200)	4.5892 (+56)	4.5439 (+11)	4.5405 (+8)	4.533
Ne	2p	0.852 (+57)	0.752 (-41)	0.8101 (+17)	0.8037 (+11)	0.793
	2s	1.931 (+149)	1.750 (-39)	1.8057 (+24)	1.7967 (+15)	1.782
Mg^{2+}:	2p	3.0068 (+56.9)	2.9217 (-28.2)	2.9572 (+7.3)	2.9537 (+3.8)	2.9499
	2s	4.4827	4.3283	4.3632	4.3589	
Mg	3s	0.253 (-28)	0.267 (-14)	0.272 (-9)	0.280 (-1)	0.281
	2p	2.282 (+162)	2.117 (-3)	2.141 (+21)	2.137 (+17)	2.12
Ar	3p	0.591 (+12)	0.563 (-16)	0.581 (+2)	0.579 (≈0)	0.579
	3s	1.277 (+202)	1.111 (+36)	1.087 (+12)	1.065 (-10)	1.075
	3s		1.840	1.578	1.544	
σ_{rms} [mH]		81.4	29.3	13.7	10.6	

TABLE IV: Ionization energies obtained with Hartree-Fock, second-order perturbation theory for the self-energy, FTDAc and with the full Faddeev-RPAc (in Hartrees). All results are extrapolated from the cc-p(C)VQZ and cc-p(C)V5Z basis sets (see Table III). The deviations from the experiment (indicated in parentheses) and the *rms* errors are given in mHartrees. The experimental energies are from Ref. [51, 52].

IV. CONCLUSIONS AND DISCUSSION

We have performed microscopic calculations of total and ionization energies in order to assess the accuracy of the Faddeev RPA approach for light atoms. The FRPA is an expansion of the many-body self-energy that makes explicit the coupling between particles and collective excitations. This formalism includes all contributions from perturbation theory up to third order, which is crucial for a correct prediction of IEs for outer-valence electrons in atomic and molecular systems. At the same time, it also includes full resummations of RPA diagrams necessary to screen the long-range Coulomb interaction in extended systems [5, 6]. While the FRPA completely includes the ADC(3) theory, it had never been tested for very small systems where violation of the Pauli Principle—that are inherent to the RPA method—may hinder satisfactory results. We find that this is not the case and the FRPA is accurate even for the two-electron problem.

In general, FTDAc/ADC(3)c and FRPAc give very similar results for the lightest systems while the inclusion of ground-state correlations via RPA theory leads to small but systematic improvements as the atomic number increases. For total binding energies, their difference is negligible in the He and Be atoms while the FRPAc yelds ≈5 mH more correlation energy for atomic numbers Z≥10. Except for the lightest atoms, 99% of the the total correlation energy is normally recovered and the total

energies obtained agree well with CCSD (as expected from the estimates for ADC(3) in Ref. [21]). The discrepancies with the experimental data are also within the errors estimated for the extrapolation to the basis set limit. The only notable exception is the neutral Be atom, for which the small gap at the Fermi surface complicates the extraction of the correlation energy. In this case, the discrepancy obtained with respect to the experiment appears to be mostly due to deficiencies in the basis set. However, a smaller fraction of it is probably related to missing correlations and/or to the lack of full self-consistency in the FRPAc (HF reference states were used).

Similar trends are found for the ionization energies. For the two-electron cases, He and Be^{2+}, FRPAc does not introduce improvements with respect to FTDAc/ADC(3)c but it gives again sensible predictions. The above problems in describing the correlations in neutral Be are also reflected in the results for the first ionization energy. For all other cases, the use of RPA shifts IEs by 2-10 mH and always brings them closer to the experiment. On average, the *rms* error for outer valence IEs lowers from 13.7 to 10.6 mH by adding RPA effects. The 3*s* orbit in Ar is found to be fragmented and configuration mixing effects between 2h1p states are required to obtain the correct ionization energy and relative intensity.

Numerically, the FRPA can be implemented as a diagonalization in 2p1h-2h1p space, implying about the same cost as an ADC(3) calculation. The present study was based on numerical codes originally developed for spherical systems [37, 45]. A first extension to molecular geometries has also been developed and first results for diatomic structures support the present conclusions [53]. Due to the inclusion of RPA excitations, the FRPA method holds promise of bridging the gap between accurate descriptions of quasiparticles in finite and extended systems. Investigating the feasibility of FRPA for larger molecules and the electron gas is therefore a priority for future research efforts. Consistent calculations of quasiparticle properties in these cases, once feasible, will also be useful for constraining functionals in quasiparticle density functional theory [54].

Acknowledgments

This work was supported by the Japanese Ministry of Education, Science and Technology (MEXT) under KAKENHI grant no. 21740213. MD acknowledges support from FWO-Flanders. DVN and MD are members of the QCMM Alliance Ghent-Brussels.

[1] T. Helgaker, *et al.*, J. Phys. Org. Chem. **17**, 913 (2004).
[2] R.J. Bartlett and M. Musiał, Rev. Mod. Phys. **79**, 291 (2007).
[3] J. Linderberg, Y. Öhrn, *Propagators in Quantum Chemistry* (Wiley, Hoboken, New Jersey, 2004).
[4] A. L. Fetter and J. D. Walecka, *Quantum Theory of Many-Particle Physics* (McGraw-Hill, New York, 1971).
[5] R. D. Mattuck, *A Guide to Feynman Diagrams in the Many-Body Problem* (MdGraw-Hill, New York, 1967).
[6] W. H. Dickhoff and D. Van Neck, *Many-Body Theory Exposed!* (World Scientific, Singapore, 2005).
[7] L. S. Cederbaum and W. Domcke, Adv. Chem. Phys. **36**, 205 (1977).
[8] W. von Niessen, J. Schirmer, and L. S. Cederbaum, Comput. Phys. Rep. **1**, 57 (1984).
[9] Zakrzewski, V. G.; von Niessen, W. J Comp Chem **14**, 13 (1993).
[10] J. V. Ortiz, *Computational Chemistry: Reviews of Current Trends, Vol. 2*, p. 1; Ed. J. Leszczyinski, (World Scientific, Singapore, 1997).
[11] D. Danovich, Encyclopedia of Computational Chemistry, vol. 2, 1190-1202, Wiley, NY, (1998).
[12] V. G. Zakrzewski, O. Dolgounitcheva, J. V. Ortiz, J. Chem. Phys. **129** 104306 (2008).
[13] O. Walter and J. Schirmer, J. Phys. B:At. Mol. Phys. **14**, 3805 (1981).
[14] L. S. Cederbaum, J. Schirmer, W. Domcke, and W. von Niessen, Adv. Chem. Phys. **65**, 115 (1986).
[15] S. Knippenberg, J.-P. François, M. S. Deleuze, Jour. Comp. Chem. **27** 1703 (2006).
[16] J. Schirmer, Phys. Rev. A **28**, 2395 (1982).
[17] J. Schirmer, L.S. Cederbaum, and O. Walter, Phys. Rev. A **28**, 1237 (1983).
[18] J. Schirmer, Phys. Rev. A **43**, 4647 (1991).
[19] F. Mertins and J. Schirmer, Phys. Rev. A **53**, 2140 (1996).
[20] M. Pernpointner, J. Chem. Phys. **121**, 8782 (2004).
[21] A. B. Trofimov and J. Schirmer, J. Chem. Phys. **123**, 144115 (2005).
[22] A. B. Trofimov, G. Stelter, and J. Schirmer, J. Chem. Phys. **117**, 6402 (2002).
[23] J. H. Starcke, M. Wormit, and A. Drew, J. Chem. Phys. **130**, 024104 (2009).
[24] L. Hedin, Phys. Rev. **139**, A796 (1965).
[25] F. Aryasetiawan, and O. Gunnarsson, Rep. Prog. Phys. **61**, 237 (1998).
[26] G. Onida, L. Reining, and A. Rubio, Rev. Mod. Phys. **74**, 601 (2002).
[27] U. von Barth and B. Holm, Phys. Rev. B **54**, 8411 (1996);
[28] B. Holm, Phys. Rev. Lett. **83**, 788 (1999).
[29] E. L. Shirley, Phys. Rev. B **54**, 7758 (1996).
[30] Y. Dewulf, D. Van Neck, and M. Waroquier, Phys. Rev. B **71**, 245122 (2005).
[31] M. Springer, F. Aryasetiawan, and K. Karlson, Phys. Rev. Lett. 1 80, 2389 (1008).
[32] P. Romaniello, S. Guyot, L. Reining, J. Chem. Phys. **131**, 154111 (2009).

[33] J. F. Dobson, in *Topics in Condensed Matter Physics*, ed. M. P. Das (Nova, New York, 1994).
[34] M. Dion, H. Rydberg, E. Schröder, D. G. Langreth, and B. I. Lundqvist, Phys. Rev. Lett. **92**, 246401 (2004).
[35] G. Román-Pérez and J. M. Soler, Phys. Rev. Lett. **103**, 096102 (2009).
[36] C. Barbieri, D. Van Neck and W. H. Dickhoff, Phys. Rev. A **76**, 052503 (2007).
[37] W. H. Dickhoff and C. Barbieri, Prog. Part. Nucl. Phys. **52**, 377 (2004).
[38] C. Barbieri *et. al.*,Phys. Rev. C **70**, 014606 (2004).
[39] C. Barbieri, Phys. Lett. B **643**, 268 (2006).
[40] C. Barbieri and M. Hjorth-Jensen, Phys. Rev. C **79**, 064313 (2009).
[41] C. Barbieri, Phys. Rev. Lett **103**, 202502 (2009).
[42] P. Danielewicz and P. Schuck, Nucl. Phys. **A567**, 78 (1994).
[43] S. Ethofer and P. Schuck, Zeitschrift für Physik **228**, 264 (1969).
[44] J. Winter, Nucl. Phys. **A194**, 535 (1972).
[45] C. Barbieri and W. H. Dickhoff, Phys. Rev. C **63**, 034313 (2001).
[46] C. Barbieri and W. H. Dickhoff, Phys. Rev. C **68**, 014311 (2003).
[47] E. R. Davidson, S. A. Hagstrom, S. J. Chakravorty, V. M. Umar, C. F. Fischer, Phys. Rev. A **A44**, 7071 (1991).
[48] S. J. Chakravorty and E. R. Davidson, J. Phys. Chem. **100(15)**, 6167 (1996).
[49] G. Martin, http://www.weizmann.ac.il/oc/martin/atoms.shtml
[50] I. E. McCarthy, R. Pascual, P. Storer, and E. Weigold, Phys. Rev. A **40**, 3041 (1989).
[51] NIST Atomic Spectra Database, NIST Standard Reference Database #78, http://physics.nist.gov/PhysRefData/ASD/in-dex.html
[52] A. Thompson *et al.*, *X-ray Data Booklet* (Lawrence Berkeley National Laboratory, Berkeley, CA, 2001), and references cited therein.
[53] Degroote *et al.*, arXiv:1010.1090 [physics.comp-ph].
[54] D. Van Neck, S. Verdonck, G. Bonny, P. W. Ayers, and M. Waroquier, Phys. Rev. A 74, 042501(2006).
[55] The augmented version of the bases (aug-cc-pVXZ) were also tested and gave no sizable improvement for the quantities being considered in this work.
[56] In the ADC language, this means adding fourth- and fifth-order terms that are introduced at the ADC(5) level.